analytical chemistry

Article

Cite This: *Anal. Chem.* 2019, 91, 14737−14742

pubs.acs.org/ac

Fe_3O_4 Nanozymes with Aptamer-Tuned Catalysis for Selective Colorimetric Analysis of ATP in Blood

Shuai Li,[†,‡,§] Xiaoting Zhao,[†,§] Xiaoxue Yu,[†] Yuqi Wan,[†] Mengyuan Yin,[†] Wenwen Zhang,[†] Bingqiang Cao,[‡] and Hua Wang*[,†]

[†]Institute of Medicine and Materials Applied Technologies, College of Chemistry and Chemical Engineering, Qufu Normal University, Qufu City, Shandong Province 273165, P. R. China

[‡]College of Physics and Engineering, Qufu Normal University, Qufu City, Shandong Province 273165, P. R. China

Supporting Information

ABSTRACT: In this work, a simple and highly selective colorimetric method has been developed for quantifying trace-level ATP using Fe_3O_4 nanoparticles (Fe_3O_4 NPs). It was discovered that Fe_3O_4 NPs could present the dramatically enhanced catalysis once anchored with ATP-specific aptamers (Apts), which is about 6-fold larger than that of bare Fe_3O_4 NPs. In the presence of ATP, however, the Apts would be desorbed from Fe_3O_4 NPs due to the Apts-target binding event, leading to the decrease of catalysis rationally depending on ATP concentrations. A colorimetric strategy was thereby developed to facilitate the highly selective detection of ATP, showing the linear concentrations ranging from 0.50 to 100 μM. Subsequently, the developed ATP sensor was employed for the evaluation of ATP in blood with the analysis performances comparably better than those of the documented detection methods, showing the potential applications in the clinical laboratory for the detective diagnosis of some ATP-indicative diseases. Importantly, such a catalysis-based detection strategy should be extended to other kinds of nanozymes with intrinsic catalysis properties (i.e., peroxidase and oxidase-like activities), promising as a universal candidate for monitoring various biological species simply by using target-specific recognition elements like Apts and antibodies.

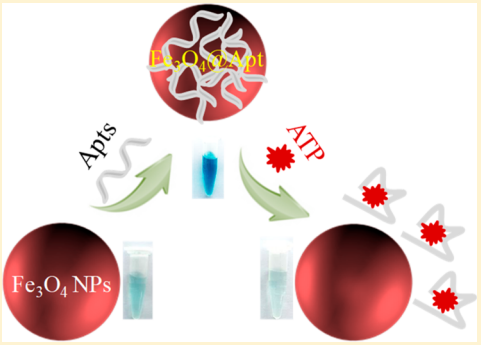

Adenosine triphosphate (ATP), an unstable high-energy phosphate complex, is one of the important signaling molecules and multifunctional nucleotides in biomedical systems.[1] It can serve as a direct source of energy required for tissues and cells to conduct their life activities like cells metabolism, known as the "molecular unit of currency" of intracellular energy transfer.[2] Especially, ATP levels in the body are closely related to some serious diseases such as Parkinson's syndrome and Alzheimer's diseases.[3,4] To date, many efficient strategies have been developed for the determination of ATP such as high performance liquid chromatography,[5] mass spectrometry,[6] fluorimetric assay,[7−9] and electrochemistry assay.[10,11] However, most of the current analysis approaches may generally suffer from some shortcomings such as operation complication, cost ineffectiveness, time consumption, and especially disability of on-site application due to bulky measurement equipment.[12] Therefore, the development of a simple, selective, sensitive, and field-deployable tactics for detecting ATP especially those in complicated biological media is an attractive but challenging target to pursue.

Moreover, the rapid development of nanozymes has opened new doors for the construction of various biosensors.[13−15] As alternatives to natural enzymes, nanozymes have attracted increasing attention due to multiple advantages of low-cost, bulk-preparation, and greater stability over natural enzymes.[16,17] Presently, many nanomaterials such as carbon nanomaterials,[18] noble metals (i.e., Au and Pt),[19] and especially metal oxide nanoparticles (NPs) like Fe_3O_4 NPs[20] have been found to possess the enzyme-like catalysis activities. Among which, Fe_3O_4 NPs inherently with a weak peroxidase-like catalysis have concentrated special application interests in the fields of chemical catalysis, biomedical detection, and magnetic separation.[21] In particular, some colorimetric biosensors have been constructed for the determination of H_2O_2 and glucose using Fe_3O_4 NPs and different catalysis enhancers.[22−25] For example, Dong's group constructed 3D porous graphene/Fe_3O_4 NPs composites with enhanced catalysis activity for the glucose detection.[23] Sun et al. developed a nanozyme-based colorimetric method for H_2O_2 detection using catalytic PtPd-Fe_3O_4.[25] Nevertheless, most of the nanozymes-based sensing strategies applied for the bioanalysis of disease biomarkers such as proteins, DNAs, and small molecules may still suffer from the poor detection selectivity because of lacking specific recognition elements. Recent studies have indicated that DNAs may act as enzyme regulators to tune the catalysis of some nanozymes like Fe_3O_4 NPs and AuNPs.[26−29] For example, Vipul Bansal and coworks

Received: September 10, 2019
Accepted: October 17, 2019
Published: October 17, 2019

DOI: 10.1021/acs.analchem.9b04116
Anal. Chem. 2019, 91, 14737−14742

reported that DNAs could conduct an inhibitory effect on the catalysis activity of AuNPs because of the physical obstruction or electrostatic repulsion.[27] Liu's group, however, discovered that oligonucleotides could enhance the intrinsic enzymatic activity of Fe_3O_4 NPs by contributing to the increased enzyme−substrate affinity.[29]

Inspired by the pioneering works above, in the present work, a simple and highly selective colorimetric analysis strategy has been developed for quantifying the trace-levels of ATP by using peroxidase-like Fe_3O_4 nanozymes, with the main sensing procedure illustrated in Scheme 1. Herein, ATP-specific aptamers (Apts) with phosphate backbones were anchored onto the surface of Fe_3O_4 NPs, serving both as the catalysis enhancers of Fe_3O_4 NPs and the specific recognition elements of ATP. It was discovered that the peroxidase-like catalysis activity of Fe_3O_4 NPs could be dramatically enhanced (about 6-fold larger) once anchored with Apts. In the presence of ATP, the Apts would be desorbed from Fe_3O_4 NPs due to the Apt-target binding, resulting in the rational decrease of catalysis of Fe_3O_4 nanozymes depending on ATP concentrations. A colorimetric strategy was thereby developed and subsequently applied for the selective detection of ATP in blood with high sensitivity. To the best of our knowledge, this is the first report on the selective colorimetric analysis for ATP by taking advantage of the Apts-tuned catalysis of Fe_3O_4 nanozymes.

EXPERIMENTAL SECTION

Reagent and Chemicals. Adenosine 5′-triphosphate disodium salt hydrate (ATP), guanosine triphosphate (GTP), uridine triphosphate (UTP), cytidine triphosphate (CTP), adenosine monophosphate (AMP), adenosine diphosphate (ADP), 3,3′,5,5′-tetramethyl benzidine (TMB), sodium pyrophosphate (PPi), trisodium phosphate anhydrous (Pi), hydrogen peroxide (H_2O_2), ethylene glycol (EG), ferric chloride hexahydrate ($FeCl_3·6H_2O$), sodium acetate (NaAc), bovine serum albumin (BSA), glutathione (GSH), ascorbic acid (AA), L-cysteine (Cys), L-histidine (His), L-lysine (Lys), L-tyrosine (Tyr), L-Glycine (Gly), L-phenylalanine (Phe), L-serine (Ser), Human Serum Albumin (HSA), and Hemoglobin (Hb), and the ATP assay kit were purchased from Sigma-Aldrich. The ATP-specific aptamers (Apts) with the sequence of ACC TGG GGG AGT ATT GCG GAG GAA GGT were obtained from Sangon Biotech (Shanghai, China). All chemicals commercially available are of analytical grade. All aqueous solutions were prepared with ultrapure water (18.2 MΩ·cm, Millipore).

Scheme 1. Main Procedure and Mechanism of the Fe_3O_4@Apt-Based Colorimetric Method for Probing ATP, Including the Apts Be Anchored on Fe_3O_4 NPs and Apts Be Desorbed from Fe_3O_4 NPs

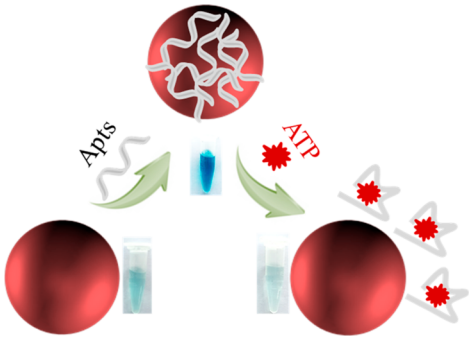

Apparatus and Instruments. Transmission electron microscopy (TEM, Tecnai G20, U.S.A.) imaging and X-ray diffraction (XRD, Bruker D8 Advance, Germany) were employed to characterize Fe_3O_4 NPs. UV−vis absorption spectra were recorded using UV-3600 spectrophotometer (Shimadzu, Japan) equipped with a thermostated holder. Colorimetric measurements were performed using Infinite M200 PRO (TECAN, Switzerland). The Zeta-potential was measured using a Zetasizer Nano ZS90 (Malvern, U.K.).

Preparation of Fe_3O_4@Apt Composites. Fe_3O_4 NPs were first prepared by a modified procedure reported previously.[30] Briefly, $FeCl_3·6H_2O$ (6.92 g) was dissolved in EG solution (140 mL) to form a clear solution by stirring vigorously, followed by addition of NaAc (9.24 g). The mixture was stirred vigorously for 30 min to obtain a uniform suspension. Then, the suspension was transferred into an autoclave (200 mL capacity), and then heated at 200 °C for 8 h. The resulting black magnetic particles were collected by magnetic separation. Subsequently, the precipitate was magnetically separated. After being washed with water and ethanol each for three times, the products were dried under vacuum at 60 °C for 12 h. Furthermore, an aliquot of ATP specific Apts (5.0 μL, 10 μM) was mixed with Fe_3O_4 NPs (95 μL, 50 μg/mL) in acetate buffer (0.20 M, pH 4.0) to be incubated for 20 min. After magnetic separation, the obtained Fe_3O_4@Apt composites were redispersed in 100 μL acetate buffer (0.20 M, pH 4.0) to be stored at 4 °C for future usage.

Catalysis Activity Measurements and Kinetic Studies. The peroxiase-like catalysis activities of Fe_3O_4 NPs, Fe_3O_4@Apt nanozymes were investigated through the catalyzing the oxidation of the substrate of TMB in the presence of H_2O_2. All the reactions were incubated in acetate buffer (0.20 M, pH 4.0), and the UV−vis absorbance values were monitored at 652 nm using the microplate reader. The experimental conditions of catalytic TMB-H_2O_2 reactions separately with Fe_3O_4 NPs and Fe_3O_4@Apt were optimized under different Apts dosages, reaction time, pH values, and temperatures. Moreover, steady state kinetic assays were comparably carried out for Fe_3O_4 NPs and Fe_3O_4@Apt, where 10 mM H_2O_2 or 0.50 mM TMB was used alternatively at a fixed concentration of one substrate versus varying concentrations of the other one. The Lineweaver−Burk plots by the double reciprocal of the Michaelis−Menten equation were thus performed to calculate the Michaelis constants (K_m) and the maximal reaction velocity (V_{max}).

Colorimetric Assays. A typical colorimetric assay for ATP was carried out as follows. An aliquot of 10 μL of ATP with different concentrations was added into 200 μL acetate buffer (0.20 M, pH 4.0) containing 50 μg/mL Fe_3O_4@Apt, 0.50 mM TMB and 10 mM H_2O_2. The mixed solution was then incubated at room temperature for 8.0 min. Afterward, the absorbance values at 652 nm were recorded using the colorimetric microplate reader. Subsequently, the assessment of ATP levels in blood samples were performed by following the same procedure above, of which the samples of ATP were prepared by spiking different concentrations of ATP in blood. All of the detections of ATP in blood samples were conducted with the approval of Animal Ethics Committee in Qufu Normal University, China.

DOI: 10.1021/acs.analchem.9b04116
Anal. Chem. 2019, 91, 14737−14742

RESULTS AND DISCUSSION

Characterization of Fe_3O_4 NPs and Fe_3O_4@Apt for ATP Sensing. Fe_3O_4 NPs were synthesized by utilizing the solvothermal method. Figure 1 shows the typical TEM image and X-ray powder diffraction patterns of Fe_3O_4 NPs. It is clearly shown that Fe_3O_4NPs could display a uniformly defined spherical shape with a size of about 500 nm in diameter (Figure 1A), as also confirmed by the SEM image shown in Figure S1 (Supporting Information, SI). The crystalline structures of Fe_3O_4 NPs were further investigated by recording their XRD patterns (Figure 1B). One can note that the marked diffraction peaks of crystalline Fe_3O_4 NPs can be obtained in good agreement with the well-established data (JCPDS 75−1609). Moreover, in order to validate the proposed mechanism for the catalysis-based ATP detection, UV−vis absorption spectra were measured comparably for Fe_3O_4 NPs before and after anchored with ATP-specific aptamers (Fe_3O_4@Apt) for sensing ATP, with the results shown in Figure 2A. Compared with Fe_3O_4 NPs (curve a), Fe_3O_4@Apt (curve b) exhibits a distinct absorption peak at 260 nm, which should belong to the characteristic absorption peak of oligonucleotides,[31] indicating that the ATP-specific Apts were successfully anchored onto the surface of Fe_3O_4 NPs by the interaction of Fe^{3+}-phosphate backbones of Apts. When ATP was introduced into the Fe_3O_4@Apt solution (curve c), the absorption peak at 260 nm disappeared, indicating that ATP-specific Apts might have been desorbed from the surface of Fe_3O_4 NPs due to the specific ATP-Apts binding. Moreover, the zeta potentials of Fe_3O_4 NPs and Fe_3O_4@Apt were investigated with the data shown in Table S1. It was found that once anchored with ATP-specific Apts, the apparent zeta potentials of Fe_3O_4 NPs would decrease from 10.30 ± 0.53 mV to −19.20 ± 0.79 mV, suggesting the successful modification of negatively charged Apts onto Fe_3O_4 NPs. Notably, the Fe_3O_4@Apt complex with negative charges of Apts might allow for more oppositely charged substrate of TMB to approach to their surfaces, resulting in the increased substrate affinity toward the increased catalysis activity, as evidenced in the kinetic studies afterward. Furthermore, the zeta-potential of Fe_3O_4@Apt could, as expected, be reduced in the presence of ATP, indicating that the detachment of ATP-specific Apts from the surfaces of Fe_3O_4 NPs. The results above validate the feasibility of the proposed colorimetric strategy for the analysis of ATP based on the Apts-tuned catalysis of Fe_3O_4 NPs and the specific ATP-Apts binding event.

Aside from the phosphate backbones of Apts, once anchored onto Fe_3O_4 NPs, DNA bases of Apts might conduct the interaction with amino groups and benzene rings-derivatized TMB substrate by hydrogen bonding and $\pi-\pi$ stacking, respectively, leading to the increased substrate affinity toward

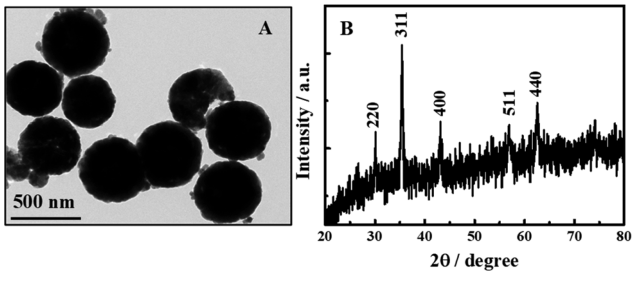

Figure 1. (A) TEM images and (B) XRD patterns of Fe_3O_4 NPs.

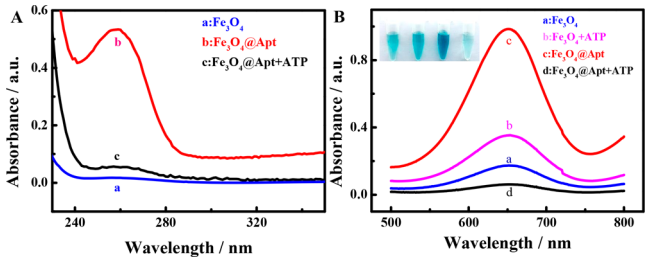

Figure 2. (A) UV−vis spectra of (a) Fe_3O_4NPs, (b) Fe_3O_4@Apt, (c) Fe_3O_4@Apt + ATP, (B) UV−vis spectra and corresponding photographs (inset) of the TMB-H_2O_2 reactions products: (a) Fe_3O_4NPs, (b) Fe_3O_4NPs+ ATP, and (c) Fe_3O_4@Apt, and (d) Fe_3O_4@Apt + ATP.

the enhanced catalytic activity of Fe_3O_4 NPs, as confirmed elsewhere.[29] Herein, such a fact was also confirmed in the experiments conducted according to the documented procedure (Figure S5), of which the results are well consistent with those reported previously.[29]

Investigation of Catalysis-Based Sensing Performances. The peroxidase-like catalysis properties of Fe_3O_4 NPs and Fe_3O_4@Apt were comparably investigated in the absence and presence of ATP by using the TMB-H_2O_2 reactions (Figure 2B). One can see that Fe_3O_4 NPs showed a little of catalysis activity for the oxidation of TMB in the presence of H_2O_2 (curve a). Moreover, the peroxidase-like catalysis activity of Fe_3O_4 NPs could be greatly enhanced (about six times higher) after coated with ATP-specific Apts (curve c), as obviously revealed by the reaction solution with a deeper blue color (Figure 2B, inset). When ATP was added into the Fe_3O_4@Apt-containing reaction solution, the specific ATP-Apts binding could trigger the desorption of the Apts from Fe_3O_4 NPs, thereby causing a decrease in the catalysis of Fe_3O_4@Apt for the TMB-H_2O_2 reactions (curve d). It is worth noting that comparing with bare Fe_3O_4 NPs, the resulted Fe_3O_4@Apt could display the even lower catalysis after adding high-level ATP (i.e.,100 μM), presumably due to the fact that the formed Apts-ATP complex with negative charges might preferentially interact with the positively charged TMB, so as to hinder its approaching to Fe_3O_4 NPs resulting in the reduced efficiency in catalyzing the TMB-H_2O_2 reactions. Besides, the effects of ATP on the peroxidase-like activity of bare Fe_3O_4 NPs were also investigated. As can be seen from Figure 2B (curve b), interestingly, the direct addition of ATP could enhance the peroxidase-like activity of Fe_3O_4 NPs to some extent, in good consistence with the investigations previously reported.[32] Yet, it indicates that the ATP-triggered decrease in the catalysis activity of Fe_3O_4@Apt should be resulted from the specific ATP-Apts binding that has caused the desorption of Apts from Fe_3O_4NPs.

Investigations on Catalysis Conditions of Fe_3O_4@Apt. The main catalysis conditions for the Fe_3O_4@Apt were investigated with the TMB-H_2O_2 reactions in comparison with bare Fe_3O_4 NPs, including the amounts of ATP-specific Apts, temperatures, pH values, and reaction time (Figure S2). First, the effects of the amounts of ATP-specific Apts on the catalysis performances of Fe_3O_4@Apt were explored. As shown in Figure S2A, higher Apts concentrations could cause greater enhancement in the catalysis of Fe_3O_4@Apt until 600 nM of Apts, over which the enhancement of catalysis might be not significant, presumably owing to the saturation of Apts anchored on Fe_3O_4NPs. This experimental data may also

DOI: 10.1021/acs.analchem.9b04116
Anal. Chem. 2019, 91, 14737−14742

demonstrate that it is the anchored ATP-specific Apts rather than free ATP-specific Apts in solution that have increased the catalysis activity of Fe_3O_4 NPs. In addition, the amounts of Apts anchored on Fe_3O_4 NPs were investigated by measuring the absorbance changes of Apts at 260 nm in the solutions before and after adding Fe_3O_4 NPs with known dosages. The results indicate that the average amount of Apts on a single Fe_3O_4 NP was calculated to be about 2.46×10^{-27} mol per particle (Figure S3). The temperature-dependent catalysis performances of Fe_3O_4@Apt were investigated by taking Fe_3O_4NPs as a comparison (Figure S2B). Accordingly, the developed Fe_3O_4@Apt composites exhibited the highest catalysis activities at about 30 °C, in good consistence with that of bare Fe_3O_4 NPs. Furthermore, the pH value-dependent catalysis of Fe_3O_4@Apt was comparably studied, revealing that for Fe_3O_4@Apt and bare Fe_3O_4 NPs should conduct the more effective catalysis at lower pH values ideally as pH 4.0 (Figure S2C). It also indicates that the introduction of ATP-specific Apts should induce no change in the pH-dependent trend of catalysis activity, but has increased their activities at each of pH values. That is, the modification of ATP-specific Apts can extend the catalytic applications of Fe_3O_4 NPs over a wide pH range. Besides, as shown in Figure S2D, the optimal time for the catalysis reactions was found to be 8.0 min. Therefore, the catalysis reactions should be carried out under the optimal conditions of Apts concentration of 600 nM, 30 °C, pH 4.0, and reaction time of 8.0 min. Besides, in order to explore the possible effects of H_2O_2 on the Apts attachments on Fe_3O_4 NPs, the fluorimetric measurements of FITC-labeled Apts onto Fe_3O_4 NPs were performed in the presence of H_2O_2 with varying concentrations. One can note from Figure S4A that H_2O_2 might conduct no significant inhibition on the Apts attachments onto Fe_3O_4NPs, except for the ones at very high concentrations (i.e., 1.0 M), which should not be attempted under the testing conditions. Similarly, as shown in Figure S4B, TMB may also exert no apparent effect on the modification of the Apts onto the surfaces of Fe_3O_4 NPs.

Studies on Steady-State Catalysis Kinetics. To further compare the peroxidase-like catalysis activity of Fe_3O_4 NPs and Fe_3O_4@Apt, the steady-state kinetics studies were performed (Figures S6 and S7). Within the suitable range of H_2O_2 and TMB concentrations, the typical Michaelis–Menten curves of Fe_3O_4 NPs (Figure S6A and C) and Fe_3O_4@Apt (Figure S7A and C) were obtained. Accordingly, the apparent Michaelis–Menten parameters were calculated by the typical Lineweaver–Burk double reciprocal curves (Figures S6B and D and S7B and D). The so obtained Michaelis constant (K_m) and maximal reaction velocity (V_{max}) values were summarized in Table S2. Typically, a lower K_m value means a higher affinity of catalyst to the substrate.[33] As shown in Table S2, as for the substrate of H_2O_2, the K_m value of Fe_3O_4@Apt is about four times higher than that of Fe_3O_4 NPs, indicating that a higher H_2O_2 concentration should be required to achieve the maximal activity. Moreover, one can see that Fe_3O_4@Apt can present about three times lower K_m value than Fe_3O_4NPs for the TMB substrate, suggesting that Fe_3O_4@Apt should possess a higher affinity toward TMB. In addition, itwas noteworthy that Fe_3O_4@Apt could exhibit the higher V_{max} values than Fe_3O_4 NPs. The data above indicate that the Fe_3O_4@Apt should possess the higher catalysis activity than Fe_3O_4NPs, so as to ensure the catalysis-based colorimetric analysis of ATP afterward.

Detection Performances of the Fe_3O_4@Apt-Based Colorimetric Assay for ATP. Considering the possible interference of other kinds of substances coexisting in the complicated biological media like blood, the responses of the Fe_3O_4@Apt-based analysis method to ATP and other kinds of ions, small molecules, and proteins were comparably investigated with the results shown in Figure 3, including the additional ones shown in Figure S8. One can see from Figures 3A and S8A that the responses to other possibly co-existing substances might be negligibly low when compared with that of ATP. Moreover, it should be pointed out that the Apts may have similar affinities for ATP, ADP, and AMP. Hence, they were herein determined at the different concentrations according to their actual level ratios in blood, i.e., ADP and AMP levels can be less than 20% of that of ATP.[34] It was found that ADP and AMP could cause about 14% response of ATP, displaying little interference on the practical detection of ATP in blood. Importantly, they could display no significant effect on the ATP detection when separately mixed with ATP, as clearly shown in Figures 3B and S8B. Therefore, the developed Fe_3O_4@Apt-based colorimetric method can promise the highly selective analysis for ATP especially those in the complicated samples such as blood. Besides, the storage stability of Fe_3O_4@Apt composites were explored (Figure S9). As expected, no obvious changes was observed in the absorbance values of catalytic reaction solutions, even the Fe_3O_4@Apt composites were stored up to 6 weeks, demonstrating the long-term stability of the catalytic probes.

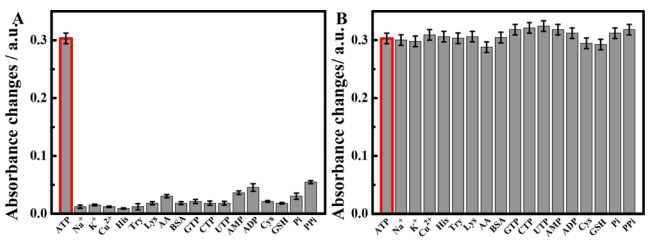

Figure 3. (A) The responses of the developed Fe_3O_4@Apt-based analysis method to different substances alone including 1.0 mM of Na^+ and K^+; 50 μM of ATP, Cu^{2+}, His, Try, Lys, AA, BSA, GTP, CTP, UTP, Cys, GSH, Pi, and PPi; and 10 μM of AMP and ADP. (B) The responses of the developed method to ATP when separately coexisting with different substances.

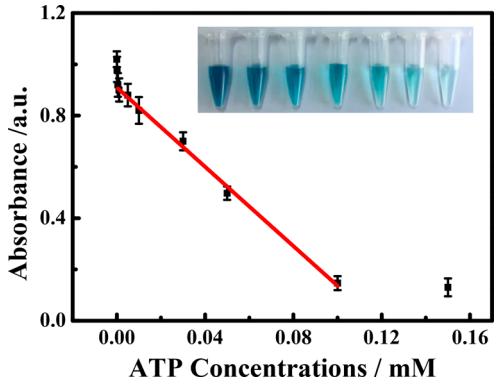

Figure 4. Calibration curves of the relationships between the absorbance responses obtained at 652 nm and different concentrations of ATP ranging from 0.50 μM to 100.0 μM (Inset: corresponding colorimetric photographs).

DOI: 10.1021/acs.analchem.9b04116
Anal. Chem. 2019, 91, 14737–14742

Table 1. Practical Analysis of ATP in Blood Samples

samples	1	2	3	4
detected (μM)	6.15 ± 0.54	6.21 ± 0.76	6.32 ± 0.43	6.37 ± 0.51
added (μM)	10.00	20.00	40.00	80.00
total detected (μM)	15.94 ± 1.25	26.11 ± 0.94	45.83 ± 0.53	84.89 ± 0.89
RSD (%)	2.34	3.12	1.98	2.87
recovery (%)	98.69	99.62	98.94	98.28

Under the optimal conditions, the developed colorimetric strategy was employed for the detections of ATP with different concentrations in acetate buffer (0.20 M, pH 4.0) (Figure 4). It was observed that with the increasing of ATP concentrations, the absorbance values of the catalytic reaction products could gradually decrease, as more apparently exhibited in the photographs of the corresponding solutions (Figure 4, inset). A linear relationship was thus obtained for the ATP detection showing the linear concentrations ranging from 0.50 to 100 μM, with the limit of detection (LOD) of about 0.090 μM as estimated by 3σ rule.

Colorimetric Analysis of ATP in Samples. The application feasibility of the Fe_3O_4@Apt-based detection method was evaluated for the ATP samples with different concentrations spiked in human blood samples on the basis of the standard addition method (Table 1). It was found that the measured ATP concentrations could be considerably close to those of the added ATP ones. Also, the obtained recoveries of these ATP-spiked samples are in the range of 98.28−99.62%, with the relative standard deviations ranging from 1.98% to 3.12%. In addition, the results for ATP in blood obtained by the developed method were compared with these obtained by the ATP assay kit, and summarized in Table S3. A statistical calculation of t test (α = 0.05) was performed to explore the accuracy of these results. Accordingly, no significant difference of the anlaysis results was observed between the developed ATP colorimetric method and the commercial ATP assay kit. Moreover, the analysis performances of the developed colorimetric analysis strategy were investigated by comparing with other documented analysis methods, with analysis results summarized in Table S4. It is found that the developed Fe_3O_4@Apt-based method can exhibit better or comparable detection performances in terms of the detection ranges and LODs. Therefore, the developed Fe_3O_4@Apt-based colorimetric method can allow for the selective detections of ATP in the complicated samples like blood.

CONCLUSIONS

In summary, a simple colorimetric biosensing strategy has been developed for the quantification of ATP with high selectivity and sensitivity. The proposed ATP sensor exploits the inherent peroxidase-like catalysis activity of Fe_3O_4 NPs by combining with the high specificity of ATP-specific Apts. It was found that Fe_3O_4NPs could present the greatly improved catalysis activity once anchored with ATP-specific Apts, which was about 6-fold larger than that of bare Fe_3O_4 NPs. In the presence of targeting ATP, the Apts-target binding event would trigger the structural changes of Apts so as to be desorbed from the Fe_3O_4 NPs surface, leading to the rationally lowering catalysis activities depending on the ATP concentrations. Moreover, the developed colorimetric analysis strategy was applied for the direct detection of ATP showing a good linearity in the ATP concentration range of 0.50−100 μM with the detection limit of 0.090 μM, which detection performances are comparably better than those of most of the other colorimetric methods documented. It can feature some specific advantages such as high specificity, visual read-out, fast response (8.0 min.), and no requirement of expensive instruments. Therefore, this colorimetric ATP analysis method holds great potential of applications in the clinical laboratory for the diagnosis of some ATP-indicative diseases such as Parkinson's syndrome and Alzheimer's diseases. More importantly, such a catalysis-based detection proposal should be extended as a universal bioanalysis format for other kinds of nanozymes to be widely applied for the analysis of various biological species simply by using target-specific recognition elements like Apts and antibodies.

ASSOCIATED CONTENT

Supporting Information

The Supporting Information is available free of charge on the ACS Publications website at DOI: 10.1021/acs.analchem.9b04116.

SEM image of Fe_3O_4 NPs; Zeta-potential test; optimization of Fe_3O_4@Apt-based colorimetric conditions; the average amount of Apts anchored on a single Fe_3O_4 NP; the effects of H_2O_2 and TMB on the modification of Apts onto Fe_3O_4 NPs; the DNA bases-depending enhancement of enzyme catalytic activity; the steady-state kinetic assays and their corresponding double reciprocal plots of Fe_3O_4 NPs and Fe_3O_4@Apt; the kinetic parameters of Fe_3O_4 and Fe_3O_4@Apt; the selectivity experiments; the stability tests of Fe_3O_4Apt; ATP determined by the ATP assay kit; and the comparison of colorimetric results among different ATP-analysis methods (PDF)

AUTHOR INFORMATION

Corresponding Author

*Phone: +86 537 4456306. Fax: +86 537 4456306. E-mail: huawang@qfnu.edu.cn. Web: http://wang.qfnu.edu.cn.

ORCID

Bingqiang Cao: 0000-0002-0866-0076

Hua Wang: 0000-0003-0728-8986

Author Contributions

§These authors contributed equally to this work.

Notes

The authors declare no competing financial interest.

ACKNOWLEDGMENTS

This work is supported by the National Natural Science Foundations of China (No.21675099); Major Basic Research Program of Natural Science Foundation of Shandong Province (ZR2018ZC0129), and Key R&D Plan of Jining City (2018HMNS001), Shandong, P. R. China.

DOI: 10.1021/acs.analchem.9b04116
Anal. Chem. 2019, 91, 14737−14742

REFERENCES

(1) Cruz-Aguado, J. A.; Chen, Y.; Zhang, Z.; Elowe, N. H.; Brook, M. A.; Brennan, J. D. *J. Am. Chem. Soc.* **2004**, *126*, 6878−6879.
(2) Rao, A. S.; Kim, D.; Nam, H.; Jo, H.; Kim, K. H.; Ban, C.; Ahn, K. H. *Chem. Commun.* **2012**, *48*, 3206−3208.
(3) Huo, Y.; Qi, L.; Lv, X. J.; Lai, T.; Zhang, J.; Zhang, Z. Q. *Biosens. Bioelectron.* **2016**, *78*, 315−320.
(4) Zhang, C.; Rissman, R. A.; Feng, J. *J. Alzheimer's Dis.* **2015**, *44*, 375−378.
(5) Bobalova, J.; Bobal, P.; Mutafova-Yambolieva, V. N. *Anal. Biochem.* **2002**, *305*, 269−276.
(6) Huang, Y. F.; Chang, H. T. *Anal. Chem.* **2007**, *79*, 4852−4859.
(7) Deng, J.; Wang, K.; Wang, M.; Yu, P.; Mao, L. *J. Am. Chem. Soc.* **2017**, *139*, 5877−5882.
(8) Jun, Y. W.; Wang, T.; Hwang, S.; Kim, D.; Ma, D.; Kim, K. H.; Kim, S.; Jung, J.; Ahn, K. H. *Angew. Chem., Int. Ed.* **2018**, *57*, 10142−10147.
(9) Kim, J. H.; Ahn, J. H.; Barone, P. W.; Jin, H.; Zhang, J.; Heller, D. A.; Strano, M. S. *Angew. Chem., Int. Ed.* **2010**, *49*, 1456−1459.
(10) Xie, H.; Chai, Y.; Yuan, Y.; Yuan, R. *Chem. Commun.* **2017**, *53*, 8368−8371.
(11) Kashefi-Kheyrabadi, L.; Mehrgardi, M. A. *Biosens. Bioelectron.* **2012**, *37*, 94−98.
(12) Wang, J.; Wang, L.; Liu, X.; Liang, Z.; Song, S.; Li, W.; Li, G.; Fan, C. *Adv. Mater.* **2007**, *19*, 3943−3946.
(13) Li, S.; Zhang, L.; Jiang, Y.; Zhu, S.; Lv, X.; Duan, Z.; Wang, H. *Nanoscale* **2017**, *9*, 16005−16011.
(14) Deng, H. H.; Luo, B. Y.; He, S. B.; Chen, R. T.; Lin, Z.; Peng, H. P.; Xia, X. H.; Chen, W. *Anal. Chem.* **2019**, *91*, 4039−4046.
(15) Cheng, H.; Liu, Y.; Hu, Y.; Ding, Y.; Lin, S.; Cao, W.; Wang, Q.; Wu, J.; Muhammad, F.; Zhao, X.; Zhao, D.; Li, Z.; Xing, H.; Wei, H. *Anal. Chem.* **2017**, *89*, 11552−11559.
(16) Vazquez-Gonzalez, M.; Liao, W. C.; Cazelles, R.; Wang, S.; Yu, X.; Gutkin, V.; Willner, I. *ACS Nano* **2017**, *11*, 3247−3253.
(17) Wang, Q.; Wei, H.; Zhang, Z.; Wang, E.; Dong, S. *TrAC, Trends Anal. Chem.* **2018**, *105*, 218−224.
(18) Shamsipur, M.; Safavi, A.; Mohammadpour, Z. *Sens. Actuators, B* **2014**, *199*, 463−469.
(19) Manea, F.; Houillon, F. B.; Pasquato, L.; Scrimin, P. *Angew. Chem., Int. Ed.* **2004**, *43*, 6165−6169.
(20) Singh, N.; Savanur, M. A.; Srivastava, S.; D'Silva, P.; Mugesh, G. *Angew. Chem., Int. Ed.* **2017**, *56*, 14267−14271.
(21) Gao, L.; Zhuang, J.; Nie, L.; Zhang, J.; Zhang, Y.; Gu, N.; Wang, T.; Feng, J.; Yang, D.; Perrett, S.; Yan, X. *Nat. Nanotechnol.* **2007**, *2*, 577−583.
(22) Wang, H.; Li, S.; Si, Y.; Zhang, N.; Sun, Z.; Wu, H.; Lin, Y. *Nanoscale* **2014**, *6*, 8107−8116.
(23) Wang, Q.; Zhang, X.; Huang, L.; Zhang, Z.; Dong, S. *ACS Appl. Mater. Interfaces* **2017**, *9*, 7465−7471.
(24) Wang, H.; Li, S.; Si, Y.; Sun, Z.; Li, S.; Lin, Y. *J. Mater. Chem. B* **2014**, *2*, 4442−4448.
(25) Sun, X.; Guo, S.; Liu, Y.; Sun, S. *Nano Lett.* **2012**, *12*, 4859−4863.
(26) Hizir, M. S.; Top, M.; Balcioglu, M.; Rana, M.; Robertson, N. M.; Shen, F.; Sheng, J.; Yigit, M. V. *Anal. Chem.* **2016**, *88*, 600−605.
(27) Weerathunge, P.; Ramanathan, R.; Shukla, R.; Sharma, T. K.; Bansal, V. *Anal. Chem.* **2014**, *86*, 11937−11941.
(28) Liu, B.; Liu, J. *Chem. Commun.* **2014**, *50*, 8568−8570.
(29) Liu, B.; Liu, J. *Nanoscale* **2015**, *7*, 13831−13835.
(30) Li, R.; Li, S.; Dong, M.; Zhang, L.; Qiao, Y.; Jiang, Y.; Qi, W.; Wang, H. *Chem. Commun.* **2015**, *51*, 16131−16134.
(31) Marusic, M.; Plavec, J. *Angew. Chem., Int. Ed.* **2015**, *54*, 11716−11719.
(32) Vallabani, N. V. S.; Karakoti, A. S.; Singh, S. *Colloids Surf., B* **2017**, *153*, 52−60.
(33) Qiu, H.; Pu, F.; Ran, X.; Liu, C.; Ren, J.; Qu, X. *Anal. Chem.* **2018**, *90*, 11775−11779.
(34) Coolen, E. J.; Arts, I. C.; Swennen, E. L.; Bast, A.; Stuart, M. A.; Dagnelie, P. C. *J. Chromatogr. B: Anal. Technol. Biomed. Life Sci.* **2008**, *864*, 43−51.

DOI: 10.1021/acs.analchem.9b04116
Anal. Chem. 2019, 91, 14737−14742